Supporting Information

for

Intramolecular Photocycloaddition Reactions of Arylcyclopropane Tethered 1-Cyanonaphthalenes

Hajime Maeda,* Shoji Matsuda, and Kazuhiko Mizuno*

Department of Applied Chemistry, Graduate School of Engineering, Osaka Prefecture University, 1-1 Gakuen-cho, Naka-ku, Sakai, Osaka 599-8531, Japan

Contents

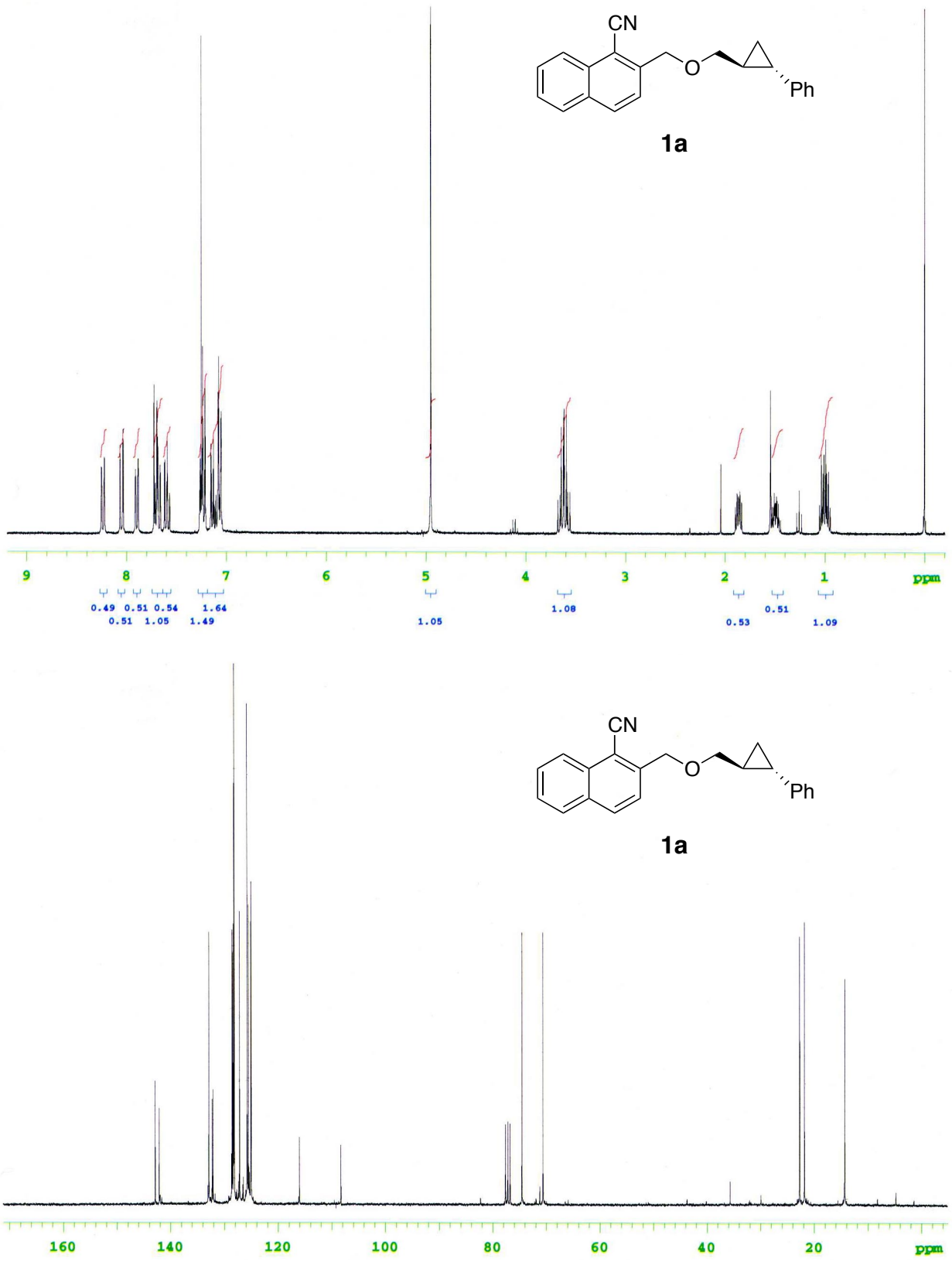

Figure S1. ^{1}H and ^{13}C NMR spectra of **1a** in $CDCl_3$.

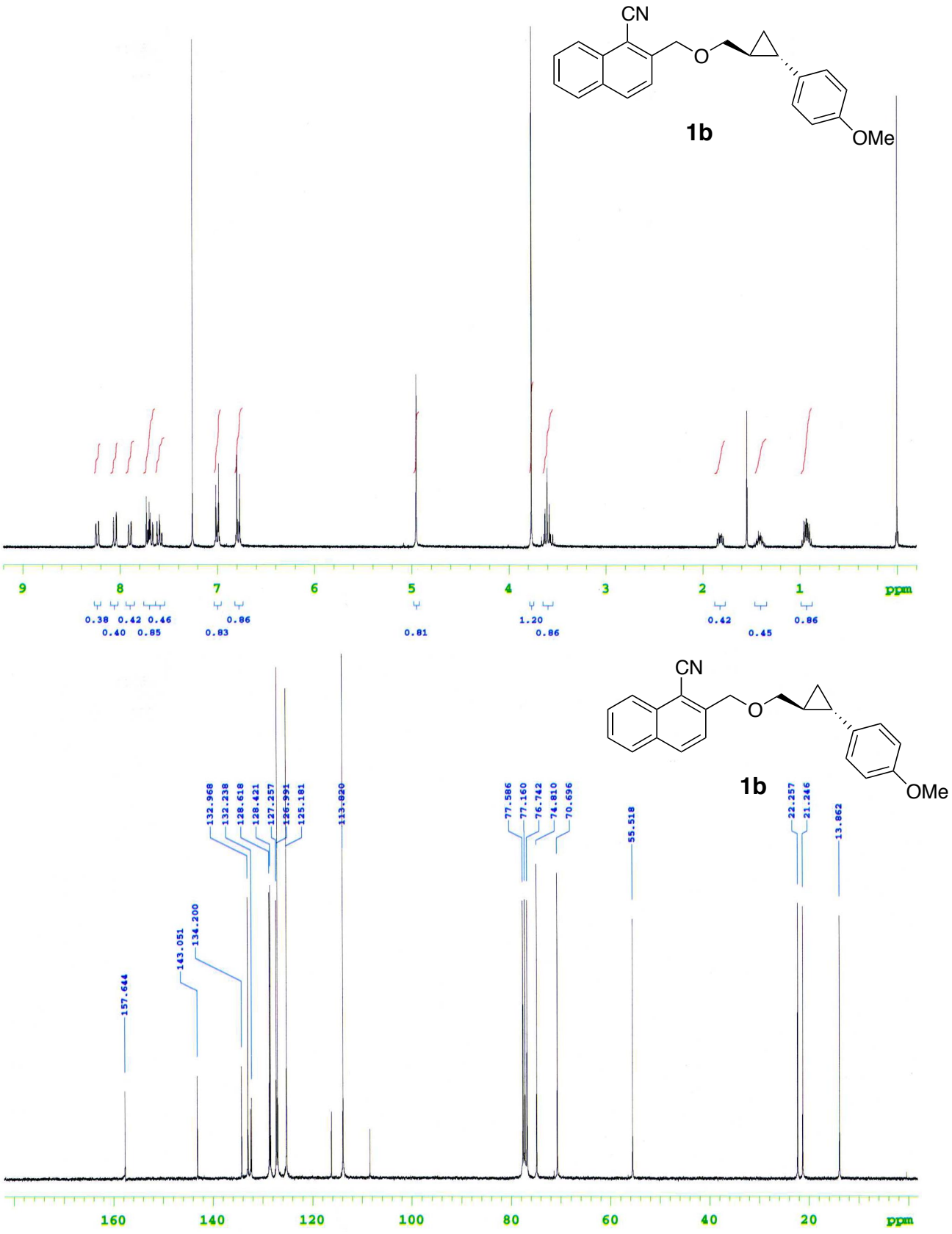

Figure S2. ^{1}H and ^{13}C NMR spectra of **1b** in $CDCl_3$.

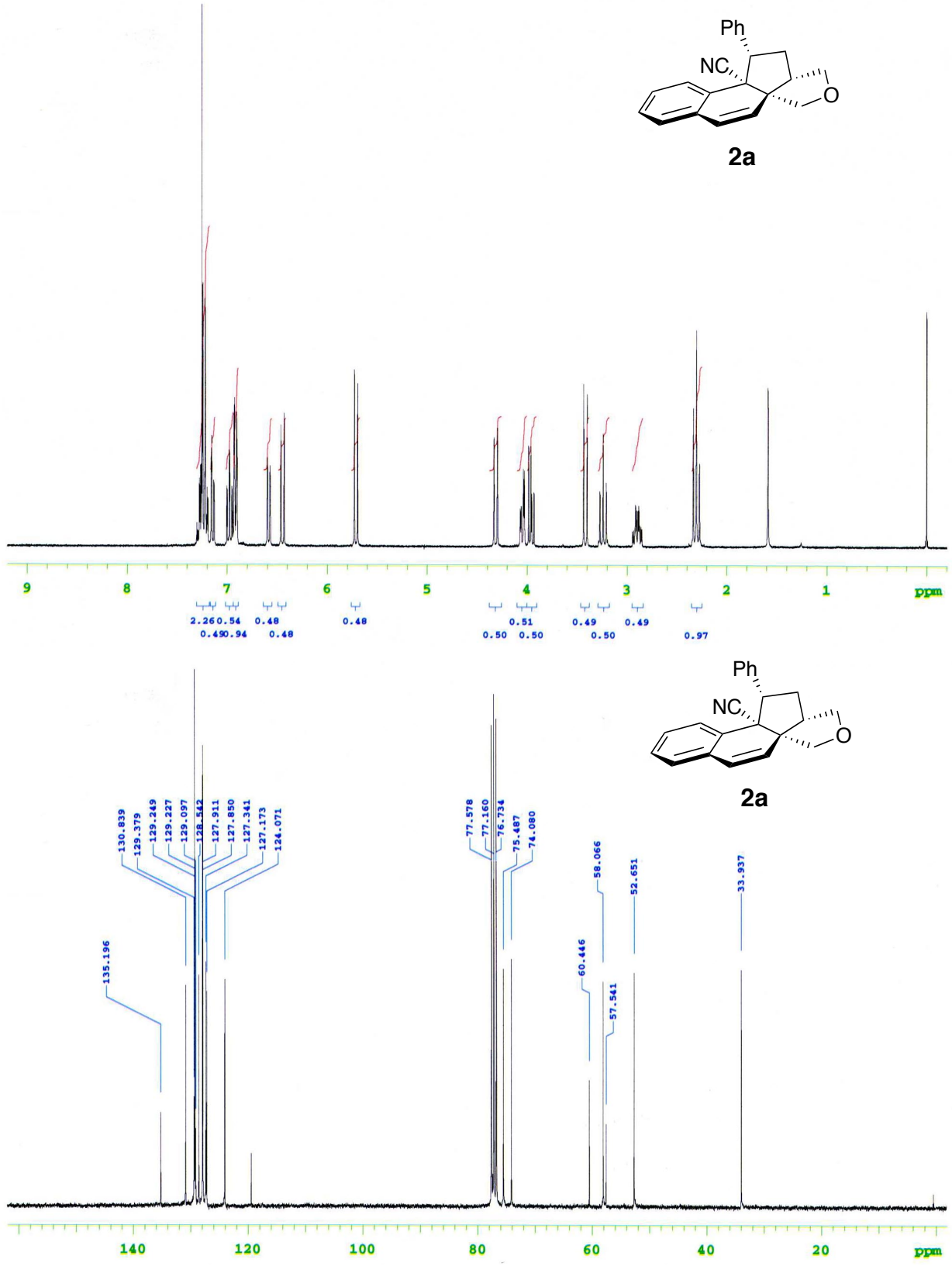

Figure S3. ^{1}H and ^{13}C NMR spectra of **2a** in $CDCl_3$.

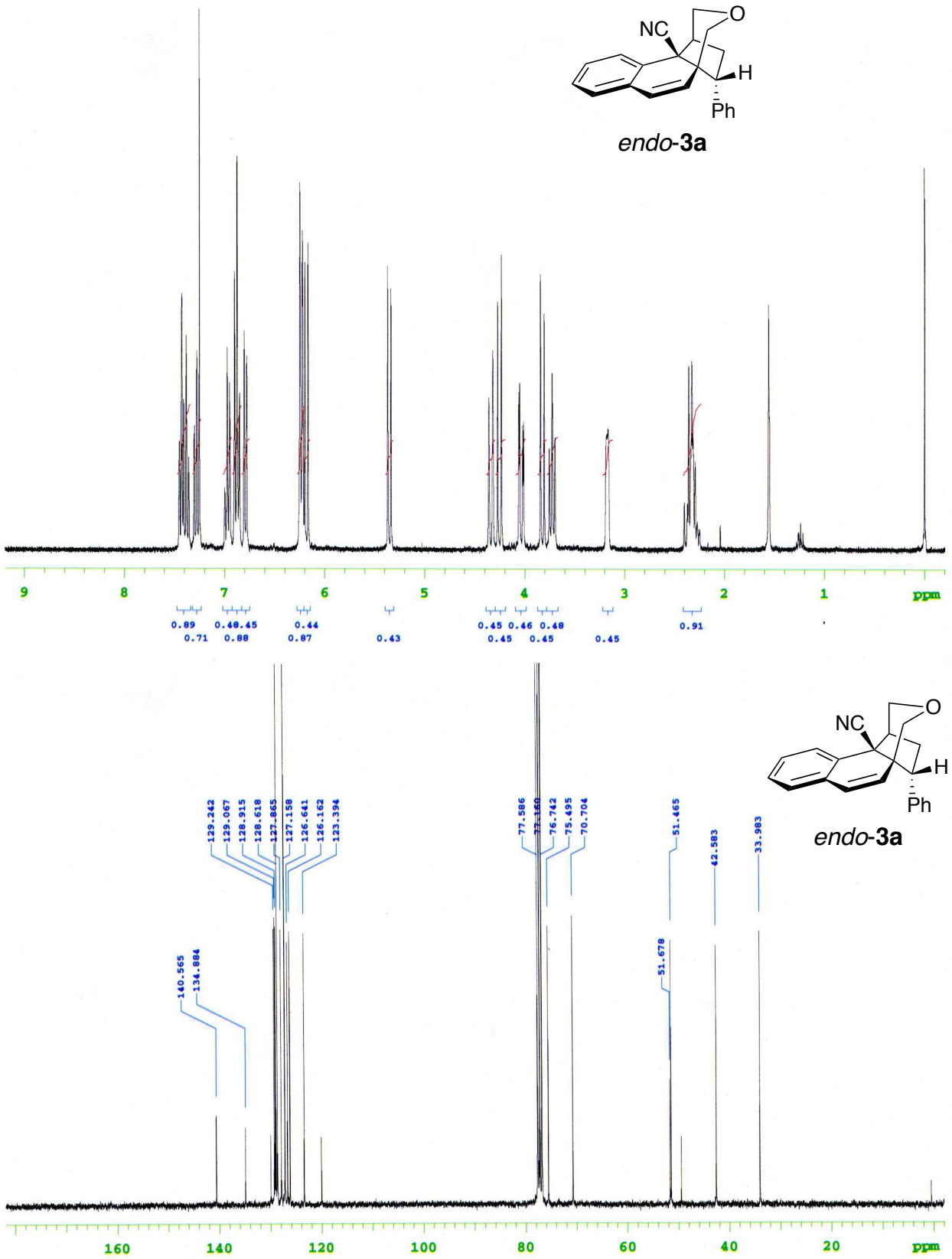

Figure S4. ^{1}H and ^{13}C NMR spectra of *endo*-**3a** in $CDCl_3$.

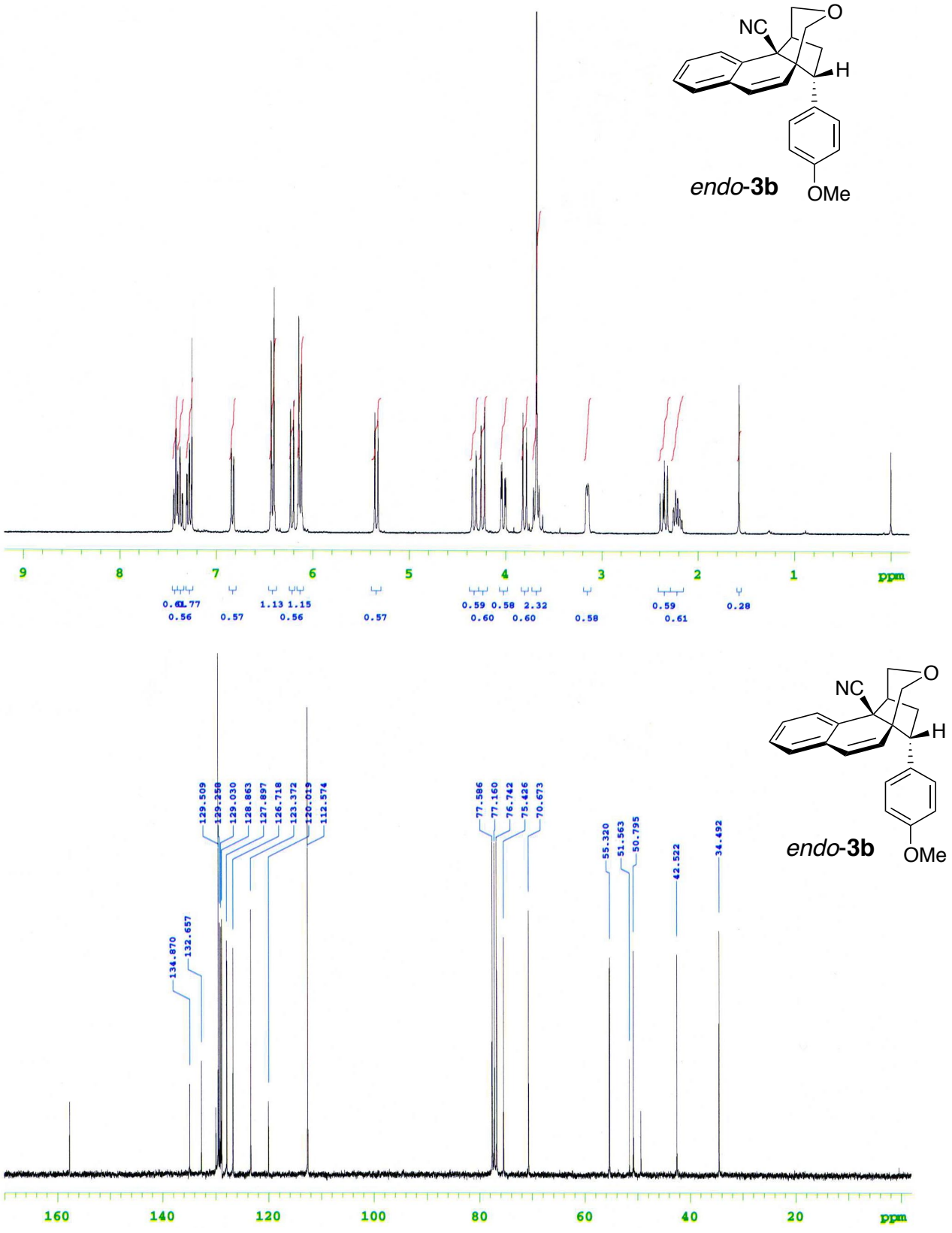

Figure S5. ^{1}H and ^{13}C NMR spectra of *endo*-**3b** in $CDCl_3$.

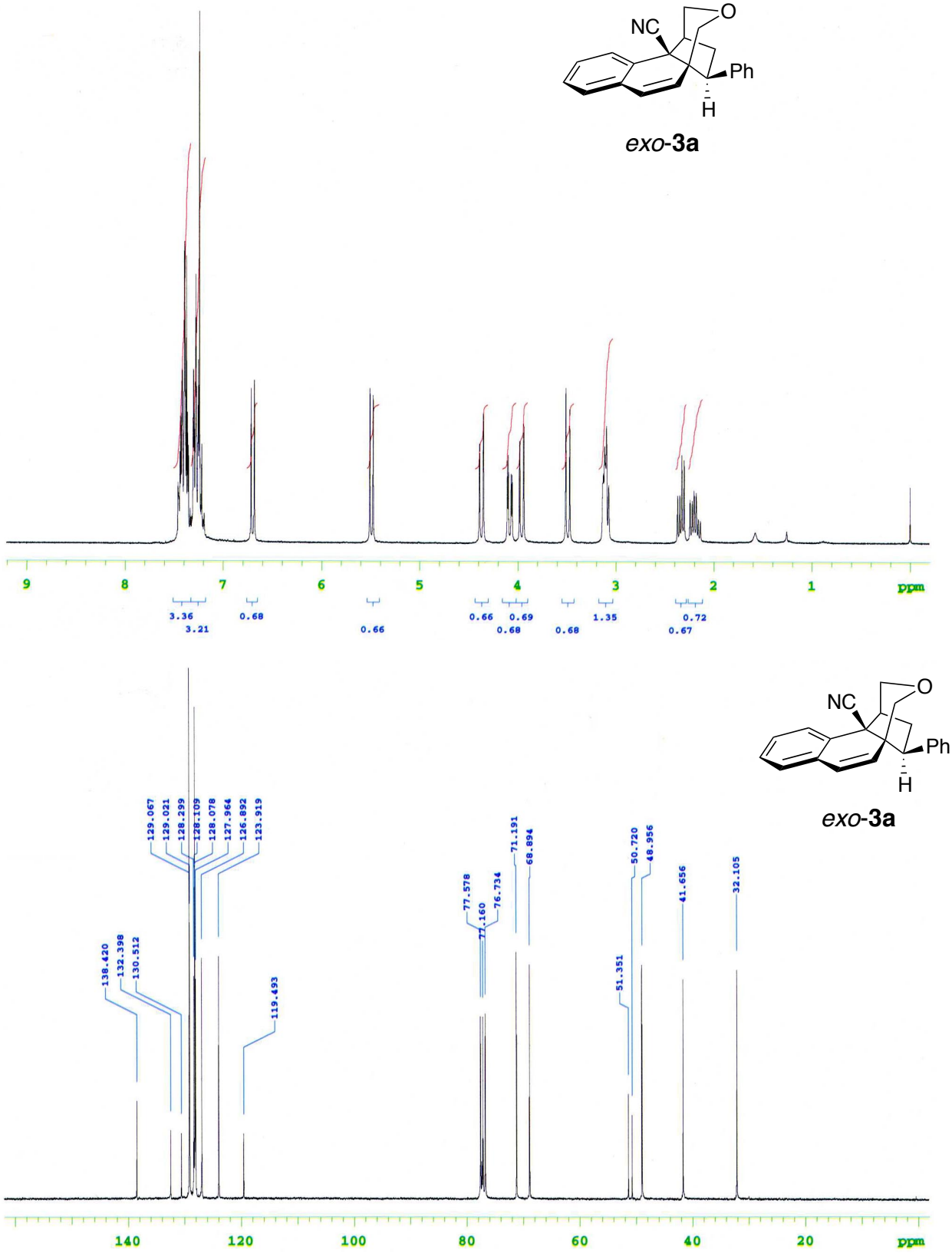

Figure S6. ^{1}H and ^{13}C NMR spectra of *exo*-**3a** in $CDCl_3$.

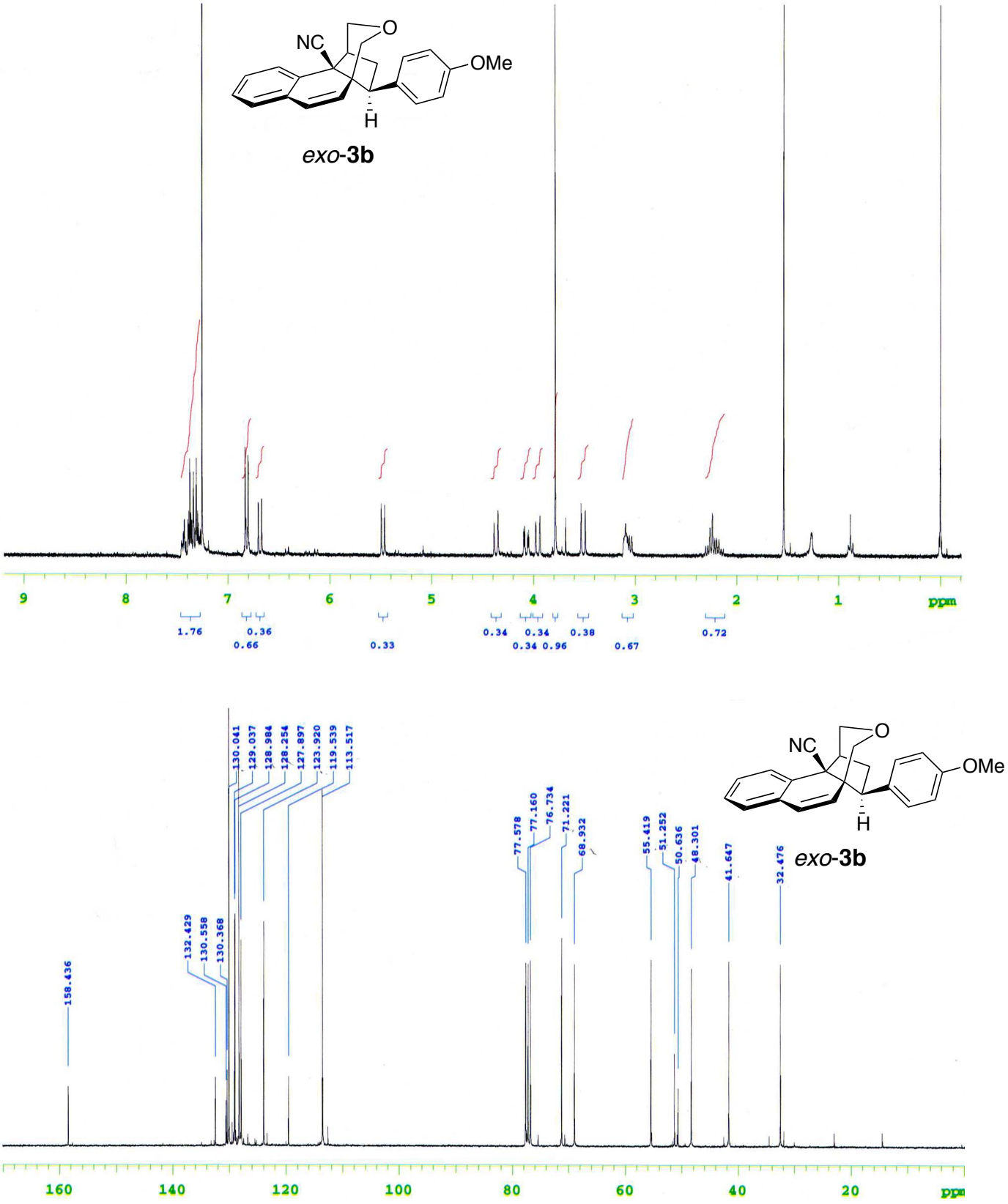

Figure S7. ^{1}H and ^{13}C NMR spectra of *exo*-**3b** in $CDCl_3$.

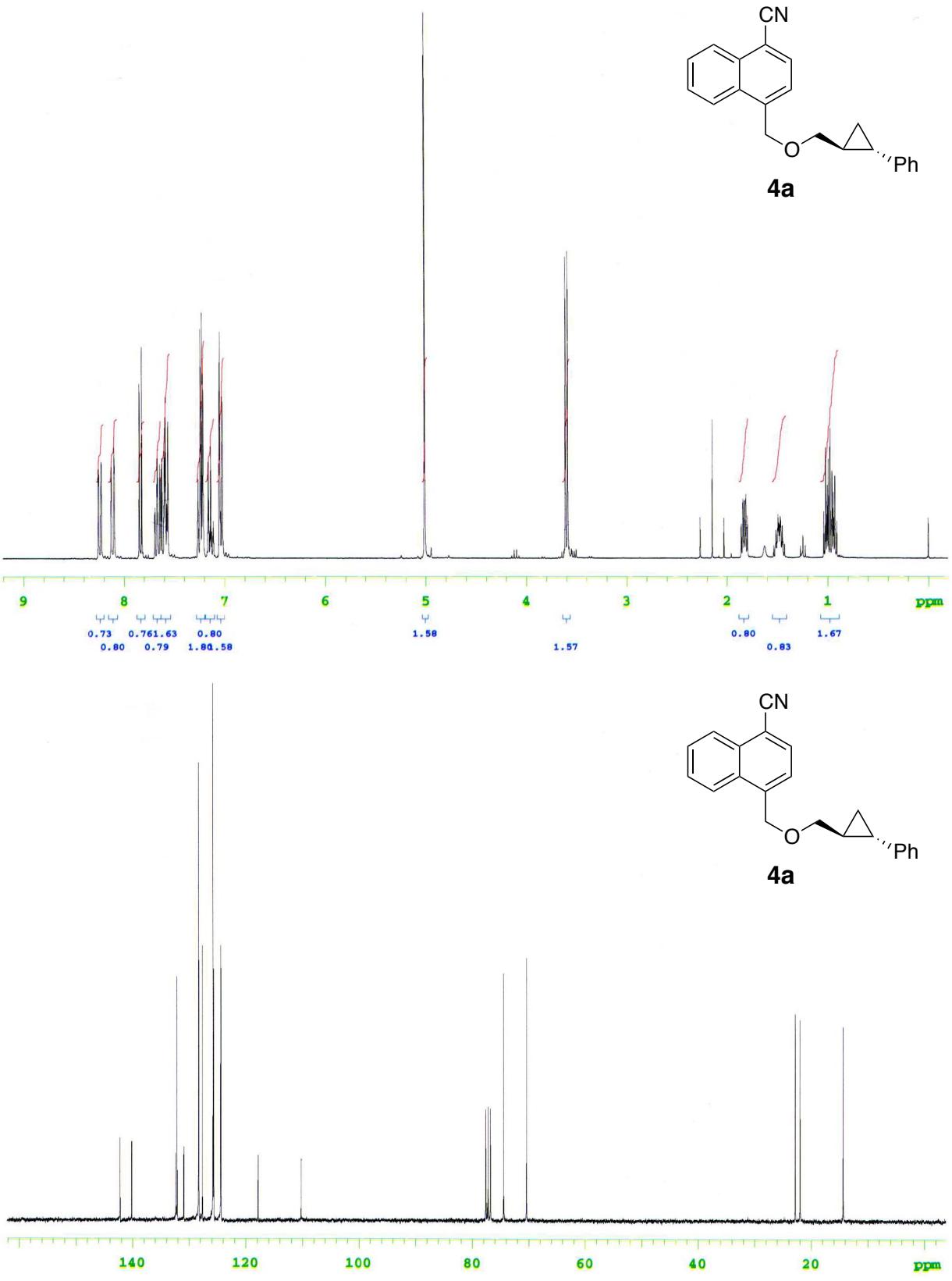

Figure S8. ^{1}H and ^{13}C NMR spectra of **4a** in $CDCl_3$.

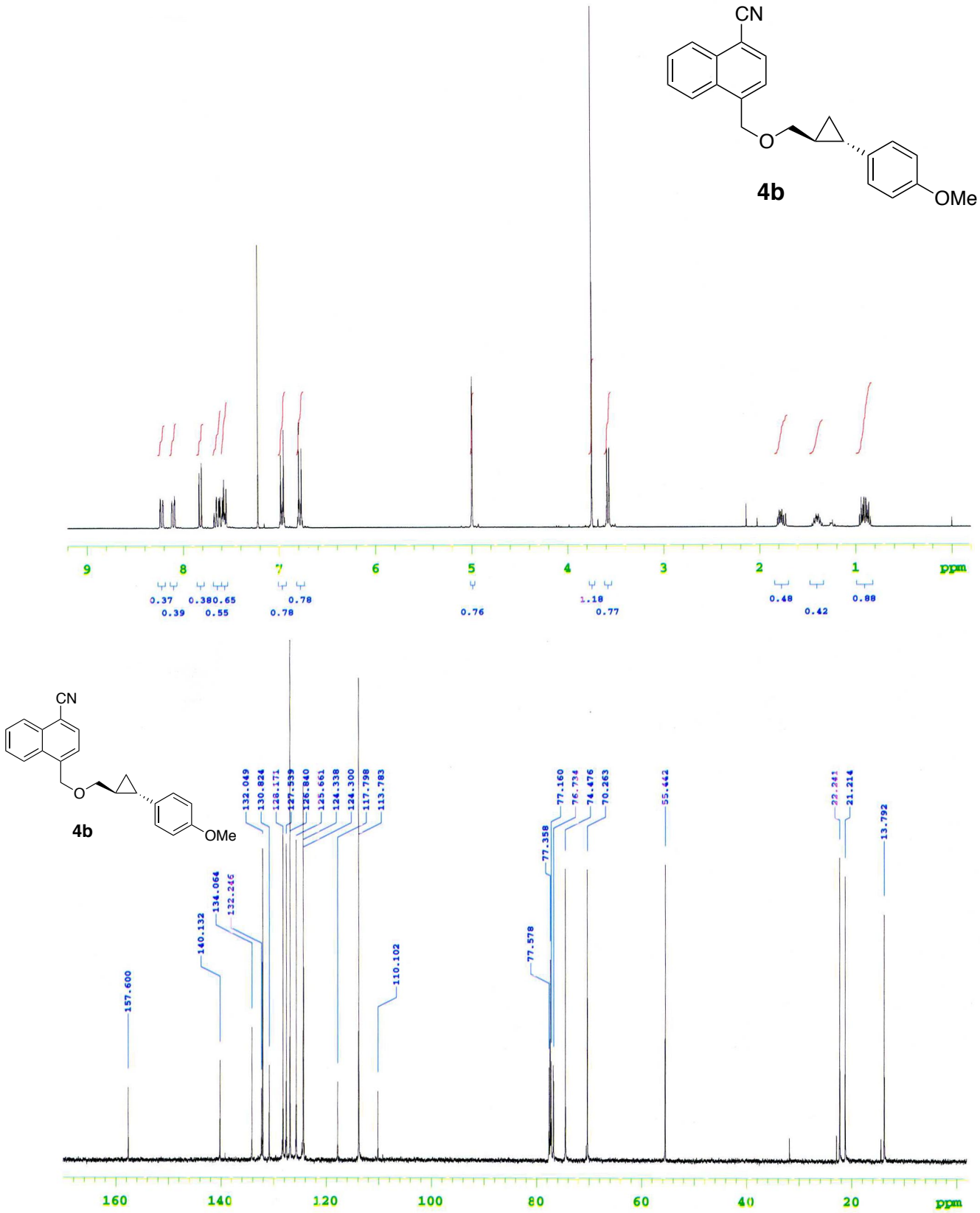

Figure S9. ^{1}H and ^{13}C NMR spectra of **4b** in $CDCl_3$.

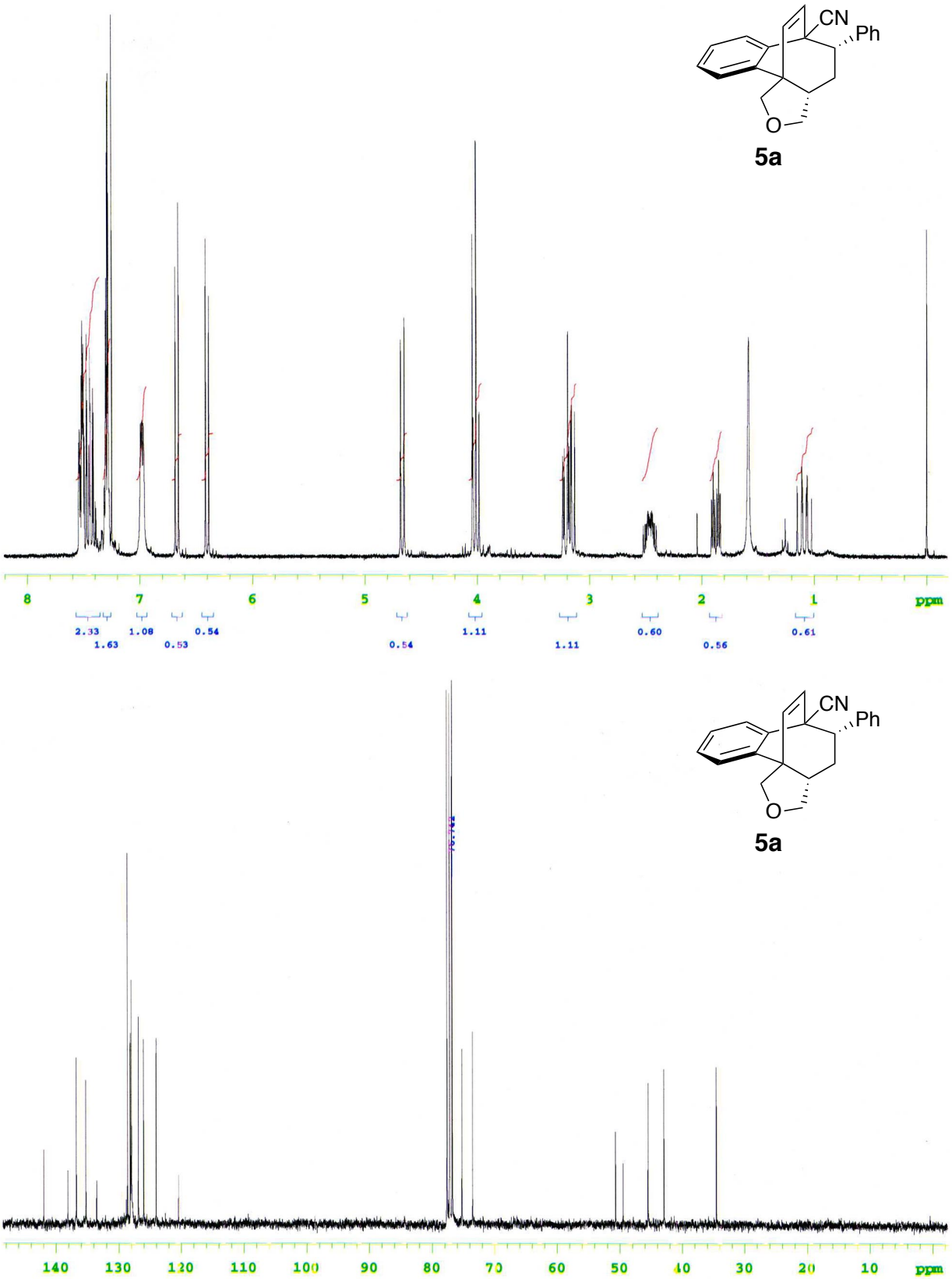

Figure S10. ^{1}H and ^{13}C NMR spectra of **5a** in $CDCl_3$.

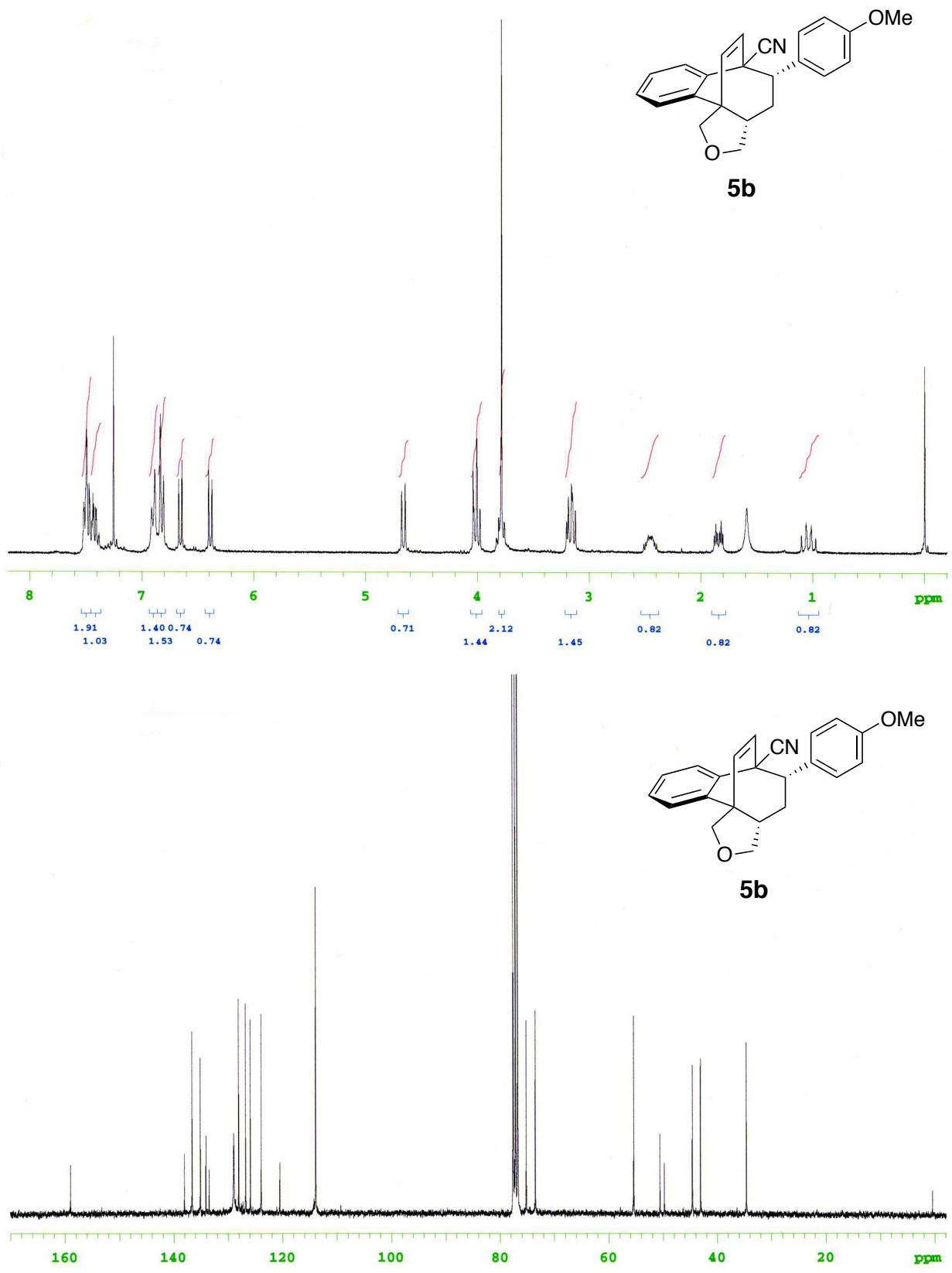

Figure S11. ^{1}H and ^{13}C NMR spectra of **5b** in $CDCl_3$.

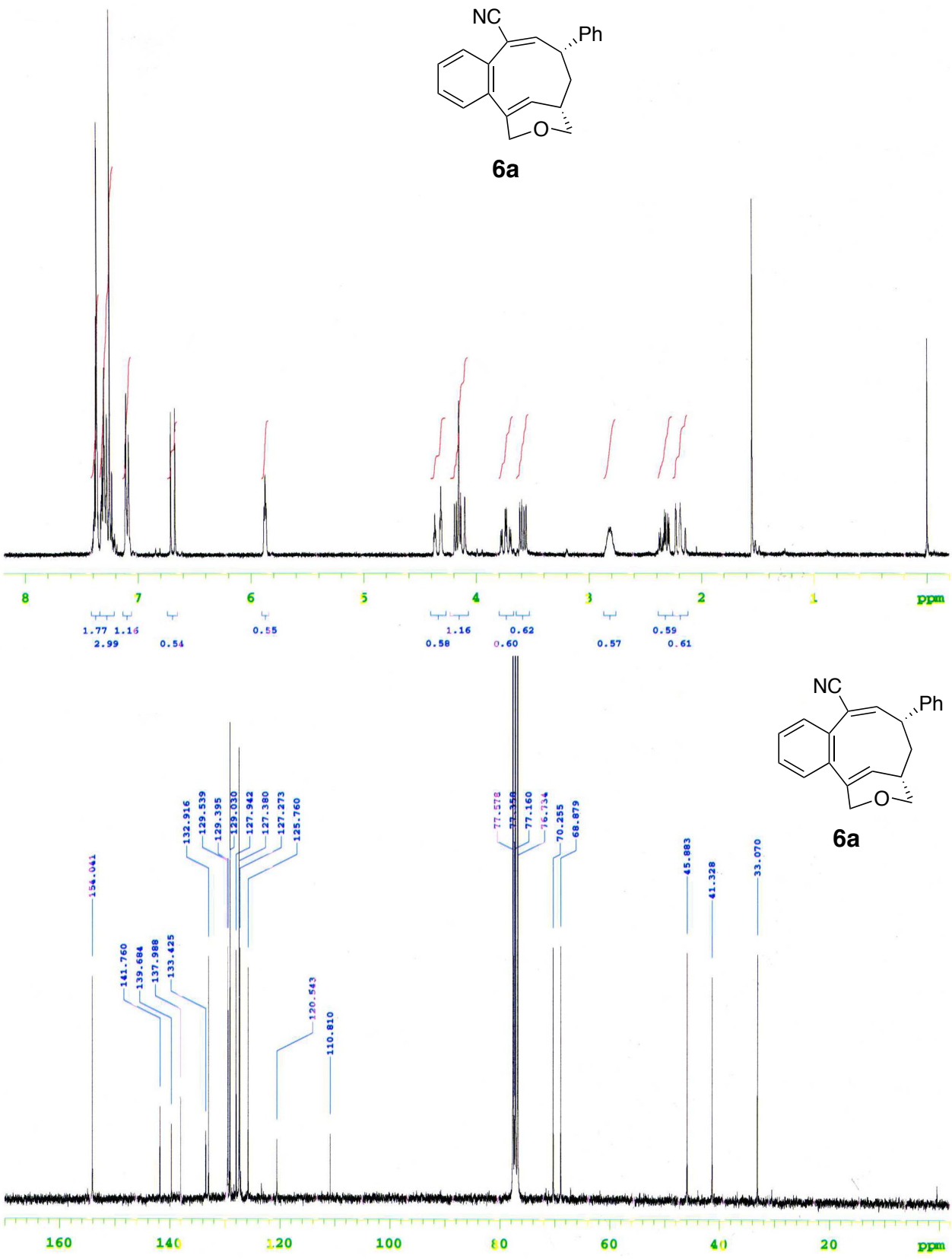

Figure S12. ^{1}H and ^{13}C NMR spectra of **6a** in $CDCl_3$.

X-ray crystallographic analysis

Single crystals were mounted on glass fibers. X-ray crystallographic data for single crystals were obtained using a Rigaku RAXIS RAPID imaging plate area detector with graphite monochromated Mo-Kα radiation. The data were collected at room temperature to a maximum 2θ value of 55. The initial phases were solved by direct methods (SIR92) and the structure was modeled by using Fourier technique. The non-hydrogen atoms were refined anisotropically. Hydrogen atoms were refined by using the riding model. All calculations were performed using the Crystal Structure crystallographic software package.

Table S1. Crystal Parameters and Refinement Matrics

	2a	*endo*-**3a**	*exo*-**3a**	**5a**	**6a**
formula	$C_{22}H_{19}NO$	$C_{22}H_{19}NO$	$C_{22}H_{19}NO$	$C_{22}H_{19}NO$	$C_{22}H_{19}NO$
mol wt	313.40	313.40	313.40	313.40	313.40
cryst dimens / mm	2.0 x 0.7 x 0.4	0.4 x 0.3 x 0.2	1.2 x 1.2 x 0.6	1.0 x 0.3 x 0.3	0.7 x 0.3 x 0.3
cryst system	monoclinic	monoclinic	monoclinic	monoclinic	monoclinic
space group	$P2_1/c$	Cc	$P2_1/c$	$P2_1/c$	$P2_1/n$
a / Å	11.3188(8)	11.1593(16)	15.2555(13)	14.9288(10)	10.9564(16)
b / Å	11.0322(8)	9.9827(16)	10.9576(8)	6.6208(6)	11.3121(13)
c / Å	13.3367(9)	30.073(4)	21.576(2)	17.0406(12)	14.0228(19)
α / deg	90	90	90	90	90
β / deg	92.0346(17)	95.774(3)	110.768(3)	104.5303(18)	90.834(4)
γ / deg	90	90	90	90	90
V / Å^3	1664.3(2)	3333.1(9)	3372.4(5)	1630.4(2)	1737.8(4)
Z	4	8	8	4	4
D_{calcd} / g cm^{-3}	1.251	1.249	1.235	1.277	1.198
temp / K	293	296	293	293	293
μ(Mo-Kα) / mm^{-1}	0.076	0.076	0.075	0.078	0.073
2θmax / deg	54.84	54.79	54.96	54.86	54.86
no. of reflections measured	3784 (Total)	6901 (Total)	7555 (Total)	3696 (Total)	3959 (Total)
	2430 (Unique)	3167 (Unique)	3918 (Unique)	2385 (Unique)	1809 (Unique)
no. observations	2448	6901	4355	2385	2227
no. variables	236	433	471	236	236
rfln/parameter ratio	10.37	15.93	9.25	10.11	9.44
R	0.0699	0.0937	0.0731	0.0632	0.1016
Rw	0.1416	0.3157	0.0907	0.0832	0.1279
goodness of fit	0.951	1.288	1.133	1.284	1.494
structure solution	SIR92	SIR92	SIR92	SIR92	SIR92

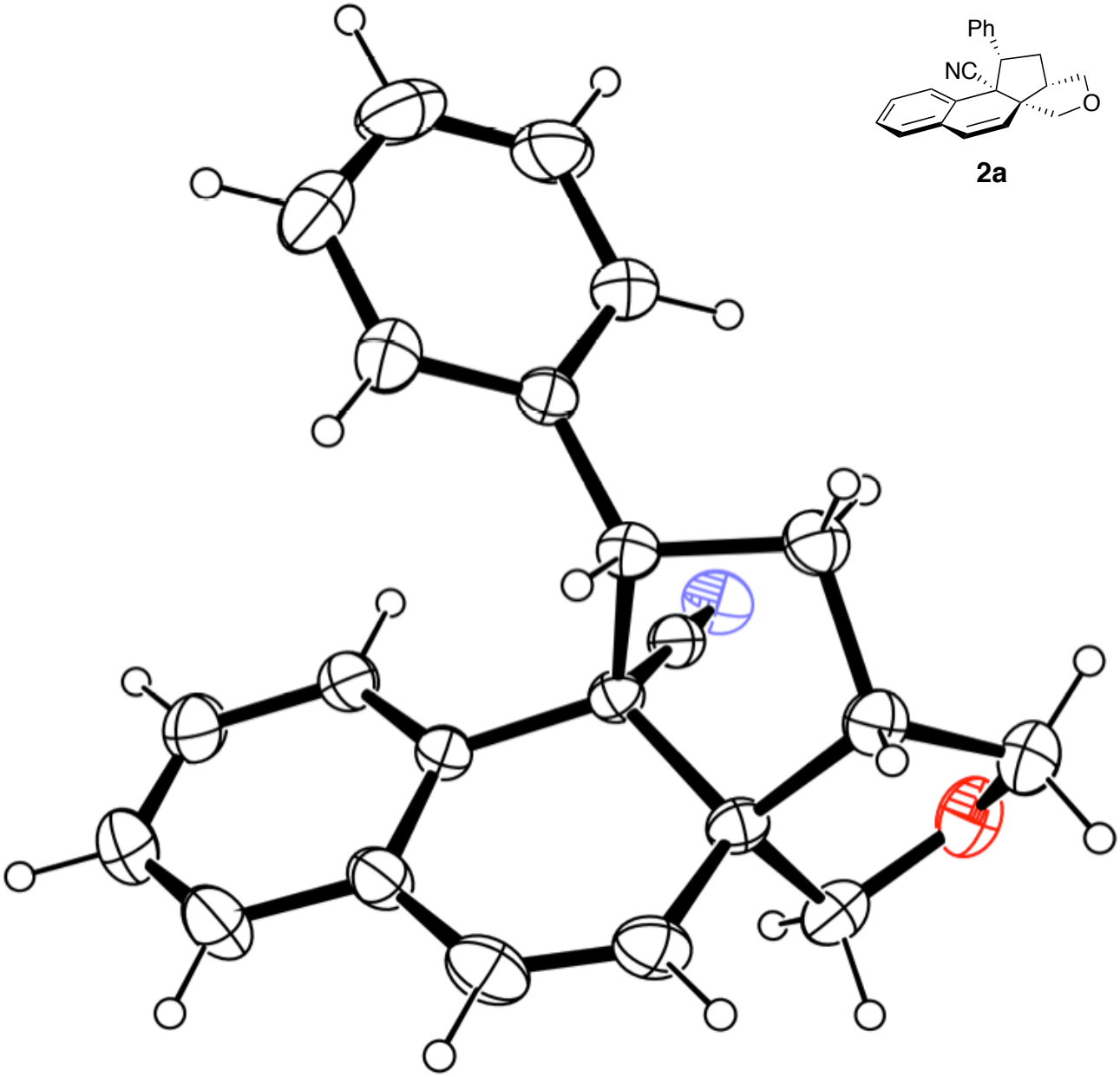

Figure S13. ORTEP plot of X-ray crystallographic data of **2a** (ellipsoids at 30% probability).

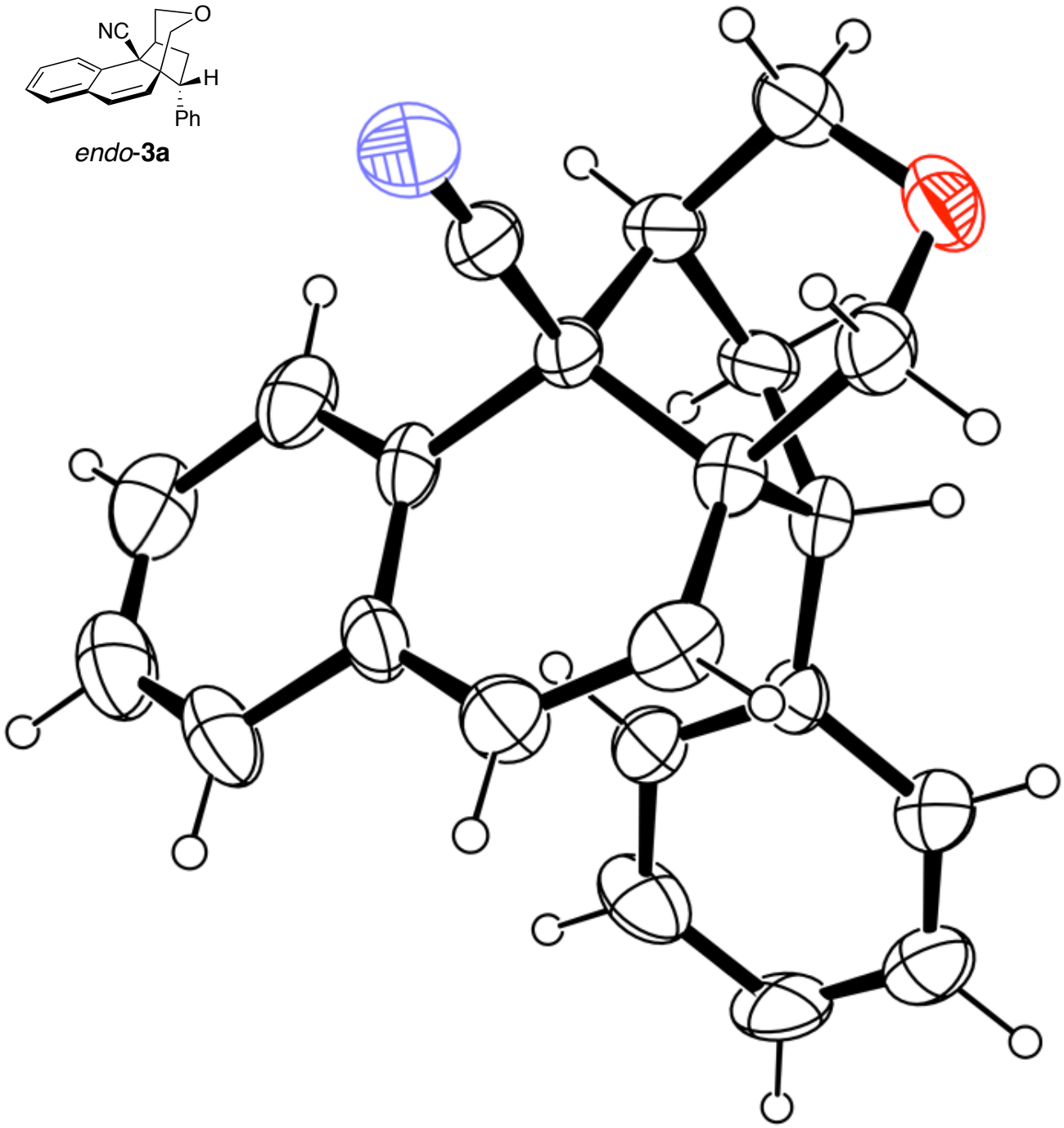

Figure S14. ORTEP plot of X-ray crystallographic data of *endo*-**3a** (ellipsoids at 30% probability).

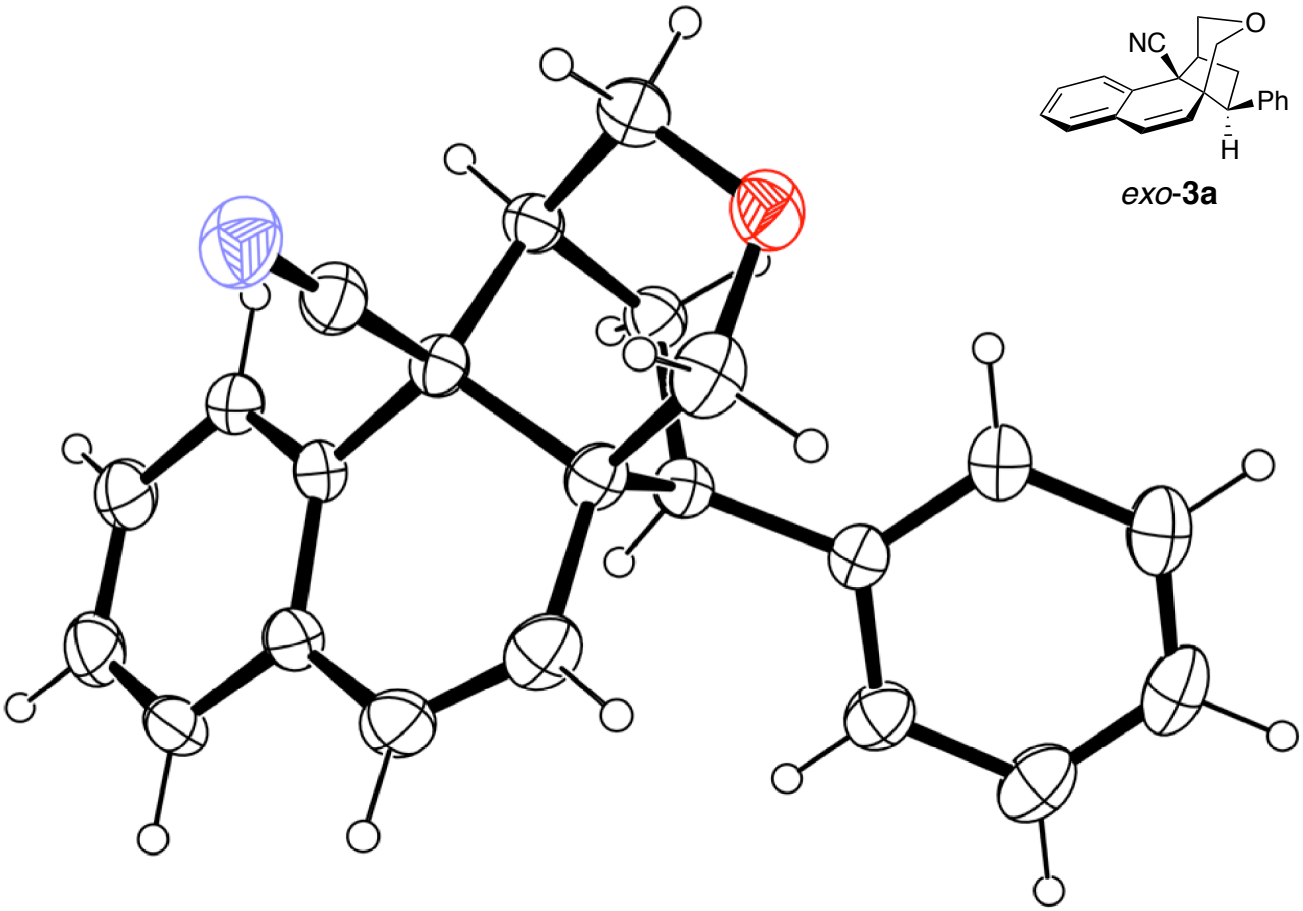

Figure S15. ORTEP plot of X-ray crystallographic data of *exo*-**3a** (ellipsoids at 30% probability).

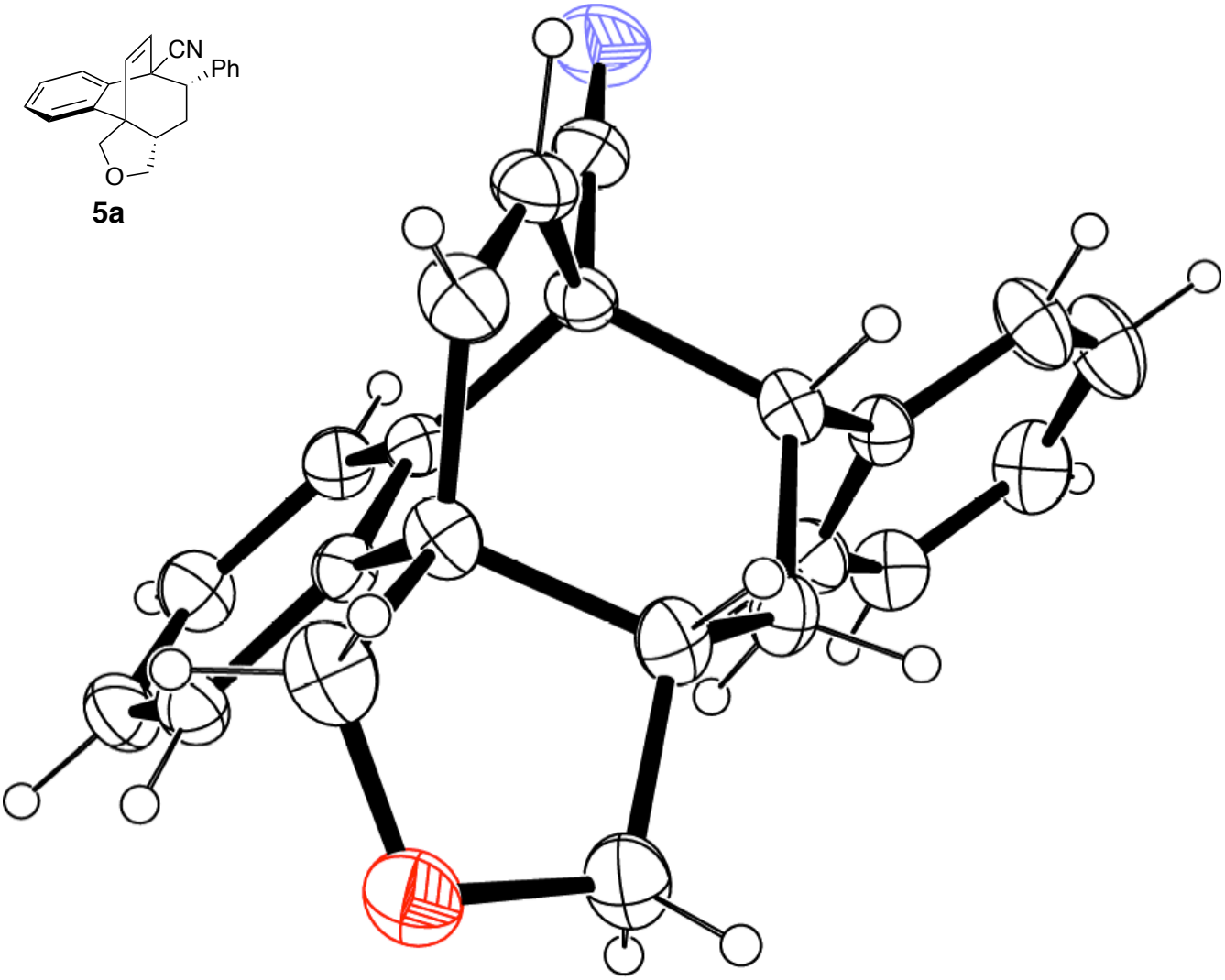

Figure S16. ORTEP plot of X-ray crystallographic data of **5a** (ellipsoids at 30% probability).

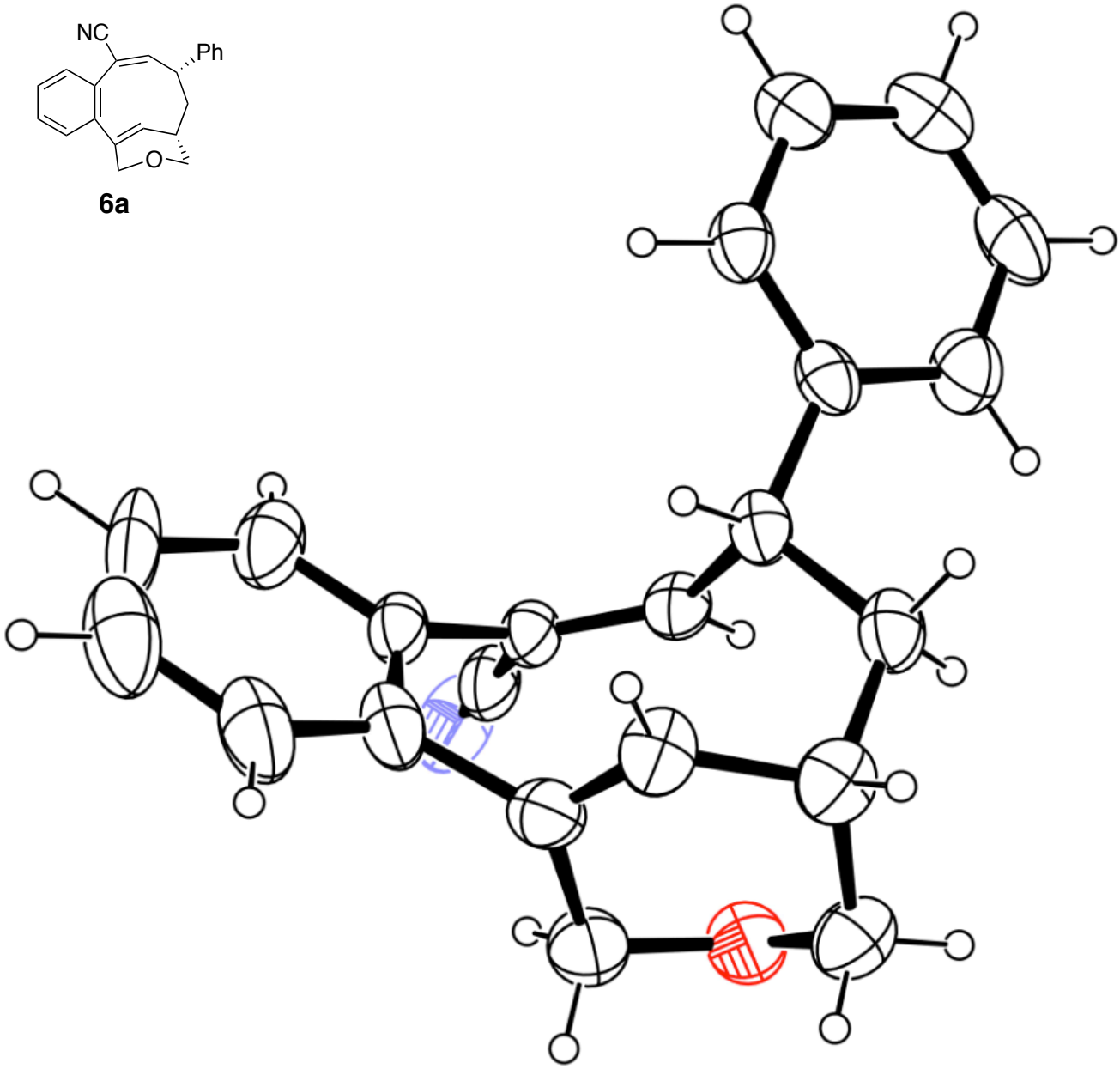

Figure S17. ORTEP plot of X-ray crystallographic data of **6a** (ellipsoids at 30% probability).